

TRIM29 Suppresses TWIST1 and Invasive Breast Cancer Behavior

Lingbao Ai^{1,2}, Wan-Ju Kim^{1,2}, Merve Alpay^{1,2}, Ming Tang^{1,2}, Carolina E. Pardo^{1,2}, Shigetsugu Hatakeyama³, W. Stratford May^{2,4}, Michael P. Kladde^{1,2}, Coy D. Heldermon^{2,4}, Erin M. Siegel^{5,6}, and Kevin D. Brown^{1,2}

Abstract

TRIM29 (ATDC) exhibits a contextual function in cancer, but seems to exert a tumor-suppressor role in breast cancer. Here, we show that TRIM29 is often silenced in primary breast tumors and cultured tumor cells as a result of aberrant gene hypermethylation. RNAi-mediated silencing of TRIM29 in breast tumor cells increased their motility, invasiveness, and proliferation in a manner associated with increased expression of mesenchymal markers (N-cadherin and vimentin), decreased expression of epithelial markers (E-cadherin and EpCAM), and increased expression and activity of the oncogenic transcription factor TWIST1, an important driver of the epithelial–mesenchymal transition (EMT). Functional investigations revealed an inverse relationship in the expression of TRIM29 and TWIST1, suggesting the existence of a negative regulatory feedback loop. In support of this relationship, we found that TWIST1 inhibited TRIM29 promoter activity through direct binding to a region containing a cluster of consensus E-box elements, arguing that TWIST1 transcriptionally represses TRIM29 expression. Analysis of a public breast cancer gene-expression database indicated that reduced TRIM29 expression was associated with reduced relapse-free survival, increased tumor size, grade, and metastatic characteristics. Taken together, our results suggest that TRIM29 acts as a tumor suppressor in breast cancer through its ability to inhibit TWIST1 and suppress EMT. *Cancer Res*; 74(17): 4875–87. ©2014 AACR.

Introduction

Currently, more than 70 members of the *Tripartite Motif* (TRIM) family (also referred to as RBCC) have been identified in humans and are typically classified because of the presence of a tripartite set of motifs, including a RING domain, one or two B-box motifs, and a coiled-coil region (1). In addition to these motifs, several family members contain additional protein–protein interaction domains such as BROMO, PHD, MATH, and SPRY domains (2). The presence of multiple protein–protein interaction motifs is thought to provide TRIM family members with significant plasticity in interaction with

various binding partners (3, 4). TRIM proteins have been implicated in a spectrum of biologic roles such as control of innate immune response, cancer, and development (for review see refs. 2, 5).

Examination of TRIM29 (aka ATDC) expression in various tumor types has found that increased expression of TRIM29 is associated with more aggressive forms of disease, including bladder (6), colorectal (7), gastric (8), lung (9, 10), and pancreatic cancer (11). Furthermore, several studies have shown an association between elevated TRIM29 expression and reduced patient survival (6, 8). In support of an oncogenic role for TRIM29, investigators found that overexpression of TRIM29 in pancreatic cancer lines promoted cell growth *in vitro* and metastatic activity *in vivo* stemming from stimulation of Wnt/ β -catenin/TCF signaling through TRIM29 binding to Dvl-2, a Wnt pathway activator downstream of the Frizzled receptor (12). Others documented that TRIM29 binds to p53 and inhibits its transcriptional activity (13).

Recently, Liu and colleagues (14) observed that knockdown of TRIM29 in the nontumorigenic MCF-10A line resulted in an increased growth rate and anchorage-independent growth, increased cell motility and invasiveness, and disrupted 3D acinar formation *in vitro*. In the MCF7 tumor line, which expresses low levels of TRIM29, expression of recombinant human TRIM29 had the opposite effect, namely, a slowing of growth and reduction in anchorage-independent growth. These findings led this group to conclude that TRIM29 functions in a growth-suppressive role in MCF7 and MCF-10A cells, although the underlying mechanisms for this effect were not reported.

¹Department of Biochemistry and Molecular Biology, University of Florida College of Medicine, Gainesville, Florida. ²UF-Health Cancer Center, University of Florida College of Medicine, Gainesville, Florida. ³Department of Biochemistry, Hokkaido University Graduate School of Medicine, Sapporo, Japan. ⁴Department of Medicine, University of Florida College of Medicine, Gainesville, Florida. ⁵Division of Population Sciences, Cancer Epidemiology Program, H. Lee Moffitt Cancer Center and Research Institute, Tampa, Florida. ⁶Department of Anatomic Pathology, H. Lee Moffitt Cancer Center and Research Institute, Tampa, Florida.

Note: Supplementary data for this article are available at Cancer Research Online (<http://cancerres.aacrjournals.org/>).

Current address for M. Alpay: Department of Biochemistry, Ankara University, Ankara, Turkey.

Corresponding Authors: L. Ai and K.D. Brown, Department of Biochemistry and Molecular Biology, University of Florida College of Medicine, Box 100245, Gainesville, FL 32610-0245. Phone: 352-273-5458; Fax: 352-392-1445; E-mail: lingbao@ufl.edu; kdbrown1@ufl.edu

doi: 10.1158/0008-5472.CAN-13-3579

©2014 American Association for Cancer Research.

Materials and Methods

Cell culture and drug treatment

All lines were obtained from the American Type Culture Collection (ATCC), authenticated, and maintained in early passages for no more than 6 months after receipt from the ATCC. Cells were treated with 5 $\mu\text{mol/L}$ (final conc) 5-aza-2'-deoxycytidine (Sigma-Aldrich) as previously published (15).

Immunoblot analysis

Nitrocellulose membranes were probed with anti-TRIM29 (sc-33151; Santa Cruz Biotechnology), E-cadherin (sc-21791), EpCAM (sc-25308), N-cadherin (sc-59987), vimentin (sc-32322), anti-Myc (#2276; Cell Signaling Technology), anti-HA (#26183; Thermo Fisher Scientific), anti-TWIST (GTX12310), or monoclonal anti-tubulin (E7; Developmental Studies Hybridoma Bank, University of Iowa, Iowa, IA). Immunoblot signals were developed using chemiluminescence.

qRT-PCR analysis

Total RNA was isolated from cultured cell lines or frozen breast tissues using TRI Reagent (Ambion). cDNA synthesis was conducted with the High Capacity RNA-to-cDNA Kit, qPCR conducted with Power SYBR Green Master Mix (Life Technologies) using an Applied Biosystems StepOnePlus thermocycler. Fold changes in relative transcript abundance were calculated with the $2^{(-\Delta\Delta C_t)}$ method (16), using GAPDH as the internal standard. Primers used for qRT-PCR are listed in Supplementary Table S1. Results shown are the mean of at least three independent experimental replicates.

Breast tumor and normal tissue specimens

Fresh-frozen breast tumors and normal breast tissues were obtained from the University of Florida Molecular Tissue Bank and the Moffitt Cancer Center Total Cancer Care Biorepository. All specimens were obtained in accordance with policies of the Institutional Review Board of the University of Florida Health Sciences Center or H. Lee Moffitt Cancer Center and Research Institute (Tampa, FL).

DNA methylation analysis

Genomic DNA was isolated from cell lines and frozen tissues with TRI Reagent. DNA was bisulfite modified using the EZ DNA methylation Kit (ZYMO) as previously outlined (17).

Quantitative DNA methylation analysis was conducted by pyrosequencing as previously described (18). A 247-bp segment of the *TRIM29* gene was amplified from bisulfite-converted DNA using primers outlined in Supplementary Table S1 and pyrosequencing conducted using the indicated sequencing primer. Bisulfite genomic sequencing (BGS) was conducted using standard protocols (19). Pyrosequencing results shown are the mean of at least three independent experimental replicates.

RNA interference

For RNAi-mediated knockdown of TRIM29, shRNA lentiviral vectors [TRCN0000016351 (#1) or TRCN0000016352 (#2)] were obtained from Open Biosystems. Lentivirus encoding shRNA or empty pLKO.1 vectors were packaged in HEK-293T cells

(ATCC) as previously outlined (15). Selection with 2 $\mu\text{g/mL}$ puromycin was conducted for approximately 1 to 3 weeks before analysis of the resultant polyclonal cell populations.

ON-TARGET plus human TWIST1 siRNA SMART pool and siRNA control were purchased from Thermo Fisher Scientific. Unless otherwise specified, cells were transfected with 200 nmol/L siRNA using Lipofectamine 2000 (Life Technologies) and 48 hours posttransfection cells were harvested and analyzed as indicated.

Recombinant protein expression

For transient protein expression, cells were transfected with pcDNA3.1-HA-ATDC (gift of Dr. E. Seto, Moffitt Cancer Center, Tampa, FL; ref. 13), pcDNA 3.1-HA-TWIST1, or Myc-Twist1-pCS2 or (gift of Dr. R. Maestro, CRO Aviano National Cancer Institute, Italy) using TurboFect Transfection Reagent (Thermo Scientific). Where indicated, the control vectors (pcDNA3.1 or Myc-GFP-pCS3) were transfected in parallel. Forty-eight hours posttransfection, cells were harvested and indicated experimentation conducted.

For stable expression of recombinant FLAG-tagged TRIM29, retrovirus was packaged in HEK-293T by cotransfecting with either pMX-puro-FLAG-TRIM29/ATDC or control pMX-puro (20), along with psPAX2 and pCL-ECO (Addgene).

In vitro cell invasion assay

Cell invasion assay was measured via modified Boyden chamber assay as described previously (21). Twenty-four hours after seeding into the top well, the bottom well was fixed and stained with Diff-Quik, invading cells photographed in 10 randomly selected fields and counted.

Cell proliferation assay

Cell proliferation was measured using CellTiter-Blue Reagent (Promega) as directed by the manufacturer. Briefly, cells were seeded in 12-well plates, and 24 and 48 hours later were washed twice with PBS and reseeded with complete growth medium containing 10% (v/v) CellTiter-Blue Reagent. Cells were incubated at 37°C for an additional 90 minutes and subsequently 100 μL of medium was removed and fluorescence measured (560-nm excitation/590-nm emission wavelength) using a BMG Labtech fluorometer. Cell proliferation at 48 hours was calculated relative to the fluorescence value recorded at 24 hours. Graphed is the result of at least three independent assays.

Transcriptional reporter assays

Human TWIST1 promoter reporter construct (pGL3-Twist-Luc) was a generous gift of Dr. Lu-Hai Wang (National Health Research Institutes, Taiwan). A 1,100-bp portion of the *TRIM29* gene proximal promoter region was amplified from human genomic DNA using primers outlined in Supplementary Table S1. The resultant amplicon was digested with NheI and XhoI at primer-encoded restriction sites, and subsequently subcloned into pGL3-Basic (Promega). A recombinant clone (pTRIM29-Luc) was confirmed by automated Sanger sequencing. Transcriptional activity was measured in transiently transfected cells using the Dual-Luciferase reporter assay system

(Promega) as previously outlined (22). Results of transcriptional reporter assays shown, represent the mean of at least three independent experiments.

Chromatin immunoprecipitation

Chromatin immunoprecipitation (ChIP) with anti-HA antibody was performed as previously outlined (15). Briefly, cells were harvested, proteins were briefly cross-linked with 1% formaldehyde (room temperature, 10 minutes), washed, and resuspended in ice-cold TEG buffer (10 mmol/L Tris, 1 mmol/L EDTA, 0.5 mmol/L EGTA, pH 8.0). Cells were sonicated on ice for 8×30 seconds, debris removed by centrifugation, and soluble chromatin was immunoprecipitated with anti-HA (Thermo Fisher Scientific) or control mouse IgG (Sigma). DNA was isolated from pelleted immunocomplexes and qPCR carried out using primers outlined in Supplementary Table S1. Shown is the mean from at least three independent ChIP assays for each indicated cell line.

Gene-expression database and statistical analysis

Gene-expression data and clinical information collected from 1,809 patients with breast cancer were downloaded from the Kaplan–Meier Plotter Breast Cancer website and indicated statistical tests conducted using IBM SPSS v20.

Results

The TRIM29 gene is a target for epigenetic silencing in cultured breast cancer cell lines

We observed that TRIM29 was only detected in the tumor lines SK–BR-3, MDA–MB-468, and nontumorigenic mammary epithelium-derived MCF-10A and immortalized human mammary epithelium cells (HMEC) by immunoblotting (Fig. 1A), consistent with a previous study (23). Furthermore, when relative TRIM29 mRNA was quantified by qRT-PCR, transcript was only detectable in these four cell lines (Fig. 1B).

We inspected the architecture of the human *TRIM29* gene locus (Fig. 1C and Supplementary Fig. S1). The *TRIM29* gene is located at 11q23.3, is comprised of 9 exons, and spans approximately 44.5 kb (Supplementary Fig. S1A). Superimposed upon exon 1 is a 664-bp GC-rich feature classified as a "CpG island" (Supplementary Fig. S1B; ref. 24). Aberrant dense cytosine methylation within CpG islands is associated with transcriptional repression and epigenetic gene silencing (25).

Given the low/absent expression of TRIM29 in many cultured breast cancer lines and *TRIM29* gene architecture, we tested for epigenetic silencing by culturing MDA–MB-231 and MCF7 cells on the global DNA demethylating drug 5-azadeoxycytidine (5-azadC). qRT-PCR analysis of RNA harvested 3 and 5 days after drug addition indicated a multifold rise in TRIM29 transcript in both lines but not in 5-azadC-treated MDA–MB-468 cells (Fig. 1D). Coordinately, 5-azadC treatment resulted in a notable increase in TRIM29 protein expression in MDA–MB-231 and MCF7 (Fig. 1E).

A pyrosequencing assay was developed to measure DNA methylation within a 35-bp region (containing 5 CpG dinucleotides) of the *TRIM29* CpG island (see Supplementary Fig. S1). MCF-10A cells contained extremely low levels of CpG methylation

(mean = 0.4%), whereas human genomic DNA methylated *in vitro* displayed near complete methylation (mean = 98.8%) within the *TRIM29* gene (Fig. 1F). Very low levels of *TRIM29* methylation were measured in SK–BR-3 and MDA–MB-468 cells (mean = 4.2% for both lines; Fig. 1G). In contrast, untreated MDA–MB-231 and MCF7 cells displayed elevated CpG methylation (mean = 74.2% and 76.2%, respectively; Fig. 1H). Consistent with gene reexpression, 5 days of 5-azadC produced a measureable decrease in *TRIM29* methylation (mean = 22.6% and 27.4%, respectively). Pyrosequencing analysis of the remaining breast tumor lines initially assayed for TRIM29 expression indicated similarly high levels of *TRIM29* gene methylation (Supplementary Fig. S2A).

BGS was also conducted on several breast cancer cell lines to examine DNA methylation density within the *TRIM29* gene. Representative data obtained from MDA–MB-231 cells, but not SK–BR-3, indicate that this line contains a pattern of dense CpG methylation within single DNA templates of the *TRIM29* gene (Fig. 1I). This finding is consistent with obtained pyrosequencing results and further supports that aberrant CpG methylation occurs within the *TRIM29* gene.

Reduced TRIM29 expression is associated with gene hypermethylation in primary breast tumors

We next examined *TRIM29* gene methylation in normal mammary tissues and primary breast tumors. Normal breast tissue samples Br-N7 and Br-N10 indicated relatively low levels of CpG methylation (mean = 12.6% and 20.6%, respectively; Fig. 2A). These levels of gene methylation are consistent with values obtained when nine additional normal human breast samples were assayed for *TRIM29* CpG methylation (mean = 18.0%, SE = 8.0%; Fig. 2B and Supplementary Fig. S2B). Primary breast tumor specimens Br-T16 and Br-T18 contained a high methylation (mean = 61.6% and 81.0%, respectively), and lower levels of CpG methylation were measured in tumor sample Br-T8 (mean = 27.2%; Fig. 2A); thus, aberrant *TRIM29* methylation occurs in primary breast tumors.

To further examine the relationship between TRIM29 mRNA abundance and *TRIM29* gene methylation, we measured TRIM29 mRNA levels in 11 normal and 30 primary breast tumor specimens (Fig. 2C and Supplementary Fig. S2C). qRT-PCR analysis revealed that 12 of the tumor samples displayed TRIM29 mRNA abundance that was equal to or greater than the geometric mean (± 1.96 SE) measured in normal breast tissues. This analysis also indicated that some breast tumors, like other tumor types (6–11), display overexpression of the *TRIM29* gene relative to normal mammary tissue. We currently do not understand the molecular basis of high TRIM29 expression in these tumors; however, the 11q23 locus is a common site of chromosomal instability in breast cancer (26). Mean *TRIM29* methylation within this group of tumors was not significant from mean methylation measured in normal breast tissues (Supplementary Fig. S2B).

qRT-PCR analysis also revealed that the majority ($n = 18$) of breast tumors displayed a significant reduction in TRIM29 mRNA relative to normal breast tissue (Fig. 2C and Supplementary Fig. S2C). Similarly, pyrosequencing indicated a significant elevation in mean *TRIM29* gene methylation compared

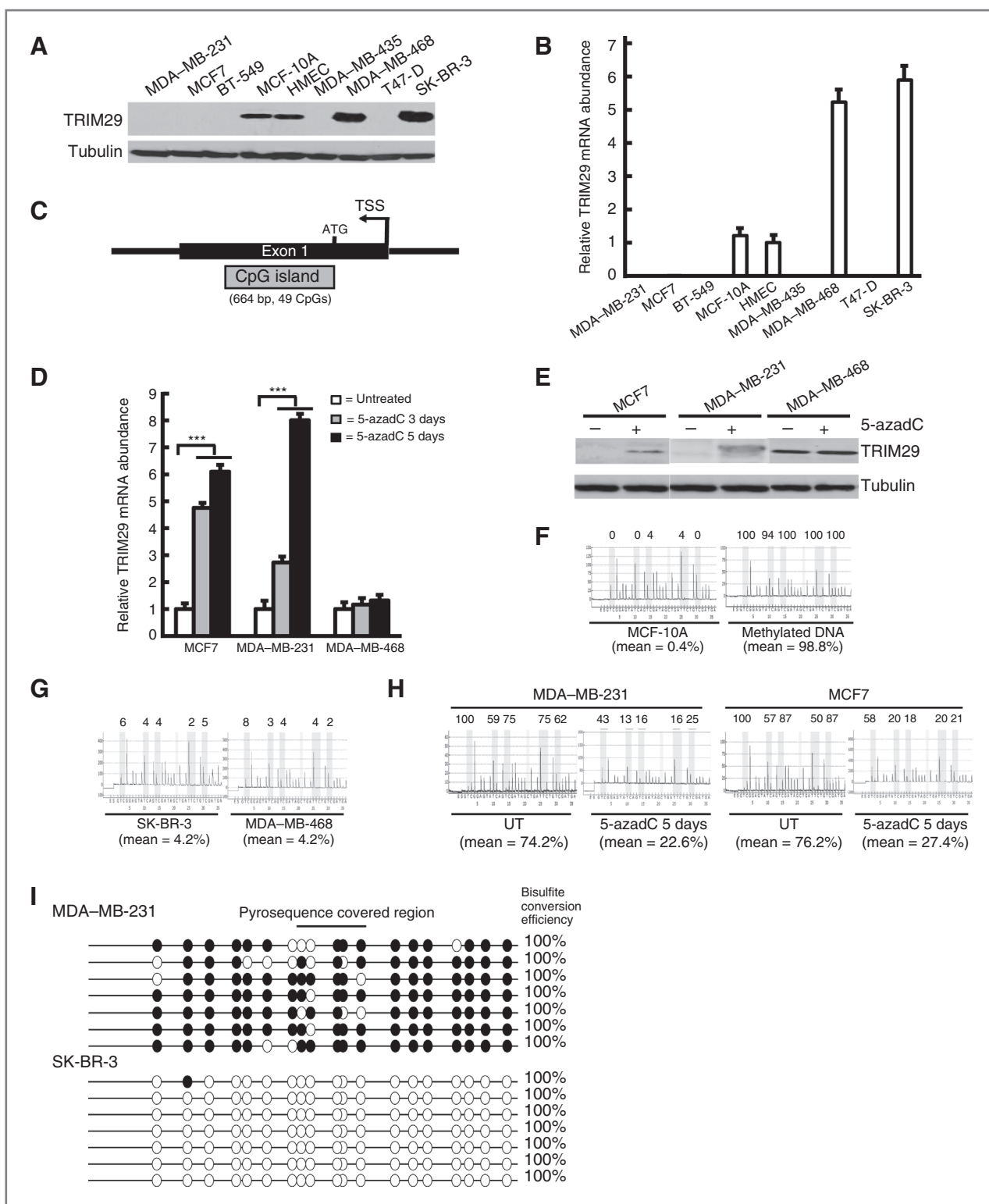


Figure 1. TRIM29 expression is epigenetically silenced in breast cancer cell lines. **A**, immunoblot analysis of lysates prepared from indicated breast tumor and nontumorigenic lines probed with anti-TRIM29 and tubulin (loading control). **B**, cell lines were assayed for relative TRIM29 transcript abundance by qRT-PCR. **C**, structure of the 5' flank and exon 1 of the human *TRIM29* gene. Indicated is the TSS, the translational start site (ATG), and the associated CpG island. **D**, MCF7, MDA-MB-231, or MDA-MB-468 cells were untreated (open bars), or treated with 5-azadC for 3 (shaded bars) or 5 (filled bars) days and TRIM29 mRNA measured by qRT-PCR. **E**, MCF7, MDA-MB-231, and MDA-MB-468 cells were cultured with or without 5-azadC for 5 days and extracts immunoblotted for TRIM29 or tubulin. (Continued on the following page.)

with normal tissues (Fig. 2B and Supplementary Fig. S2B). When relative TRIM29 mRNA and *TRIM29* gene methylation in the breast tumors with low TRIM29 mRNA levels were analyzed on a scatterplot, we observed a significant ($P < 0.001$) inverse correlation between TRIM29 mRNA levels and gene methylation (Fig. 2D). From these studies, we conclude that the *TRIM29* gene is commonly hypermethylated in cultured breast cancer cells and primary breast tumors, and is a novel target for epigenetic silencing.

Knockdown of TRIM29 results in increased breast cancer cell motility and invasiveness

The recent work of Liu and colleagues (14) showed that reduced expression of TRIM29 in MCF-10A cells altered cellular behavior. To extend these findings, we used RNAi-mediated gene knockdown to diminish expression of TRIM29 in two human breast tumors (SK-BR-3 and MDA-MB-468) and two nontumorigenic lines (MCF-10A and HMEC). Immunoblotting indicated a multifold reduction in TRIM29 when stably transduced with lentivirus encoding TRIM29-specific shRNA compared with cells transduced with control shRNA vector (pLKO.1; Fig. 3A and Supplementary Fig. S3A). We observed a notable change in cell morphology in cultures of SK-BR-3 and MDA-MB-468 cells within 2 weeks of TRIM29 knockdown using two independent shRNA vectors (Fig. 3B). Specifically, both lines acquired a spindle-like morphology commonly associated with motile cells (27). In contrast, cultures of MCF-10A or HMEC displayed a less dramatic change in morphology following TRIM29 knockdown (data not shown).

Forty-eight hours after wounding monolayer cultures, we observed increased cell migration into the wound in each TRIM29 knockdown line compared with control lines (Fig. 3C). Invasion assays on cells with and without TRIM29 knockdown were conducted using a modified Boyden chamber assay (Fig. 3D), and we measured statistically significant increases in invasive activity in each line following TRIM29 knockdown (Fig. 3E). Finally, a proliferation assay indicated that TRIM29 knockdown significantly increased cell growth rates relative to controls (Fig. 3F). These experiments reveal that TRIM29 knockdown in cultured breast tumor and nontumorigenic cell lines increases cell motility, proliferation, and invasiveness.

TWIST1 is upregulated and gene-expression patterns altered following TRIM29 knockdown

Increased invasive behavior is often linked to alterations in gene-expression patterns, resulting in downregulation of epithelial and upregulation of mesenchymal genes (27). SK-BR-3 do not express E-cadherin (28), a prominent epithelial marker, but we observed a measurable decrease in both E-cadherin protein (Fig. 4A) and transcript abundance (Fig. 4B) in MDA-MB-468 cells following TRIM29 knockdown. In contrast, no

detectable alteration in E-cadherin protein was observed in MCF-10A (Fig. 4A), but an approximately 2-fold decrease in CDH1 mRNA was measured in response to TRIM29 knockdown (Fig. 4B). EpCAM, an epithelial cell adhesion molecule, also showed decreased expression in TRIM29 knockdown SK-BR-3, MDA-MB-468 and MCF-10A cells by both immunoblotting and qRT-PCR (Fig. 4A and B, respectively).

We measured a sharp increase in protein (Fig. 4A) and mRNA (Fig. 4B) of the mesenchymal marker N-cadherin in SK-BR-3, and a more moderate increase in MCF-10A following TRIM29 knockdown. Analysis of MDA-MB-468 cells failed to detect even basal expression of N-cadherin in this cell line. Experiments indicated that TRIM29 knockdown resulted in an increase in both the vimentin protein and transcript in each cell line. In sum, although results are somewhat variable between the cells included in this study, knockdown of TRIM29 resulted in a downregulation of epithelial and upregulation of mesenchymal genes.

Such alterations in gene expression are governed, in part, by a set of basic helix-loop-helix (bHLH) transcription factors that promote acquisition of motile and invasive behavior (29). The principal bHLH proteins responsible for such alterations are SNAIL (SNAI1), SLUG (SNAI2), TWIST1, ZEB1, and ZEB2. Analysis of SNAIL, SLUG, ZEB1, and ZEB2 expression by either qRT-PCR or immunoblotting proved inconclusive; however, when extracts of SK-BR-3, MDA-MB-468, and MCF-10A cells were immunoblotted with an anti-TWIST1 antibody, we observed, in each line, increased levels of this protein associated with TRIM29 knockdown (Fig. 4C) and parallel results were obtained when qRT-PCR was used to measure TWIST1 transcript (Fig. 4D). Analysis of SK-BR-3 and MDA-MB-468 cells using two independent TRIM29 shRNA sequences also displayed increased TWIST1 protein and transcript abundance, decreased EpCAM and increased N-cadherin expression (Supplementary Fig. S3A and S3B), indicating that these effects are specific to TRIM29 knockdown.

TWIST1 and TRIM29 exhibit a reciprocal relationship

To better understand the relationship between TRIM29 and TWIST1, we transiently expressed recombinant HA-tagged TRIM29 in SK-BR-3 and MDA-MB-468 cells and observed endogenous TWIST1 levels decreased in both lines (Fig. 5A). We also observed expression of recombinant Myc-tagged Twist1 decreased endogenous TRIM29 abundance (Fig. 5B). qRT-PCR indicated that TRIM29 expression resulted in a significant drop in TWIST1 transcript and, conversely, that expression of recombinant Twist1 decreased TRIM29 mRNA (Fig. 5C).

We next transfected SK-BR-3 or MDA-MB-468 cells with TWIST1-specific or control siRNA and observed that TWIST1-specific siRNA resulted in knockdown of TWIST1 and increase

(Continued.) F, genomic DNA harvested from MCF-10A cells or human genomic DNA methylated *in vitro* was bisulfite modified and analyzed for *TRIM29* gene methylation by pyrosequencing. Shown are representative pyrograms, the percentage of methylation at each CpG analyzed, and the mean percentage of methylation over the region analyzed. G, genomic DNA was harvested from SK-BR-3 and MDA-MB-468 cells and analyzed by pyrosequencing. H, genomic DNA was harvested from untreated (UT) MDA-MB-231 and MCF7 cells or after culture with 5-azadC for 5 days and analyzed by pyrosequencing. I, representative bisulfite sequencing results from MDA-MB-231 and SK-BR-3 cells; filled, methylated CpG; open, unmethylated CpG. Indicated is the region covered by pyrosequencing (top) and bisulfite conversion efficiency (right); error bars, 1.0 SE; ***, $P < 0.001$, Student *t* test.

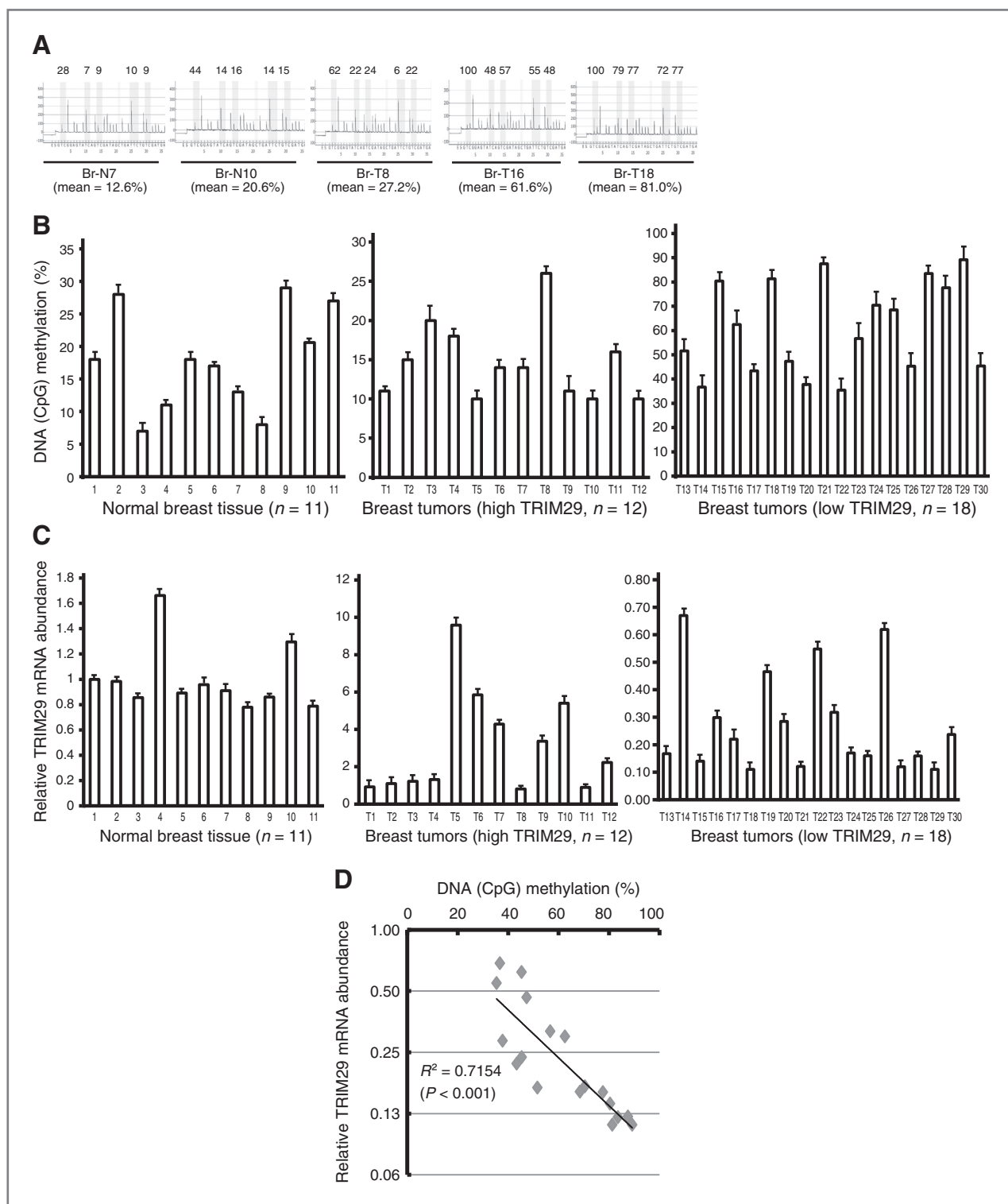


Figure 2. Aberrant hypermethylation of the TRIM29 gene is associated with reduced expression in primary breast tumors. A, genomic DNA was harvested from normal mammary tissues (Br-N7 and Br-N10) and primary breast tumor specimens (Br-T8, Br-T16, and Br-T18) and analyzed by pyrosequencing. B, TRIM29 gene methylation was measured in normal breast tissues and primary breast tumors by pyrosequencing. C, normal breast tissue and primary breast tumors were assayed for relative TRIM29 mRNA abundance by qRT-PCR. D, shown is a scatterplot graphing relative TRIM29 mRNA abundance and TRIM29 gene methylation measured within the group of 18 breast tumors with low relative TRIM29 mRNA levels. Regression line was drawn using exponential regression; indicated is the coefficient of determination (R^2) and the calculation of the P value (Spearman correlation).

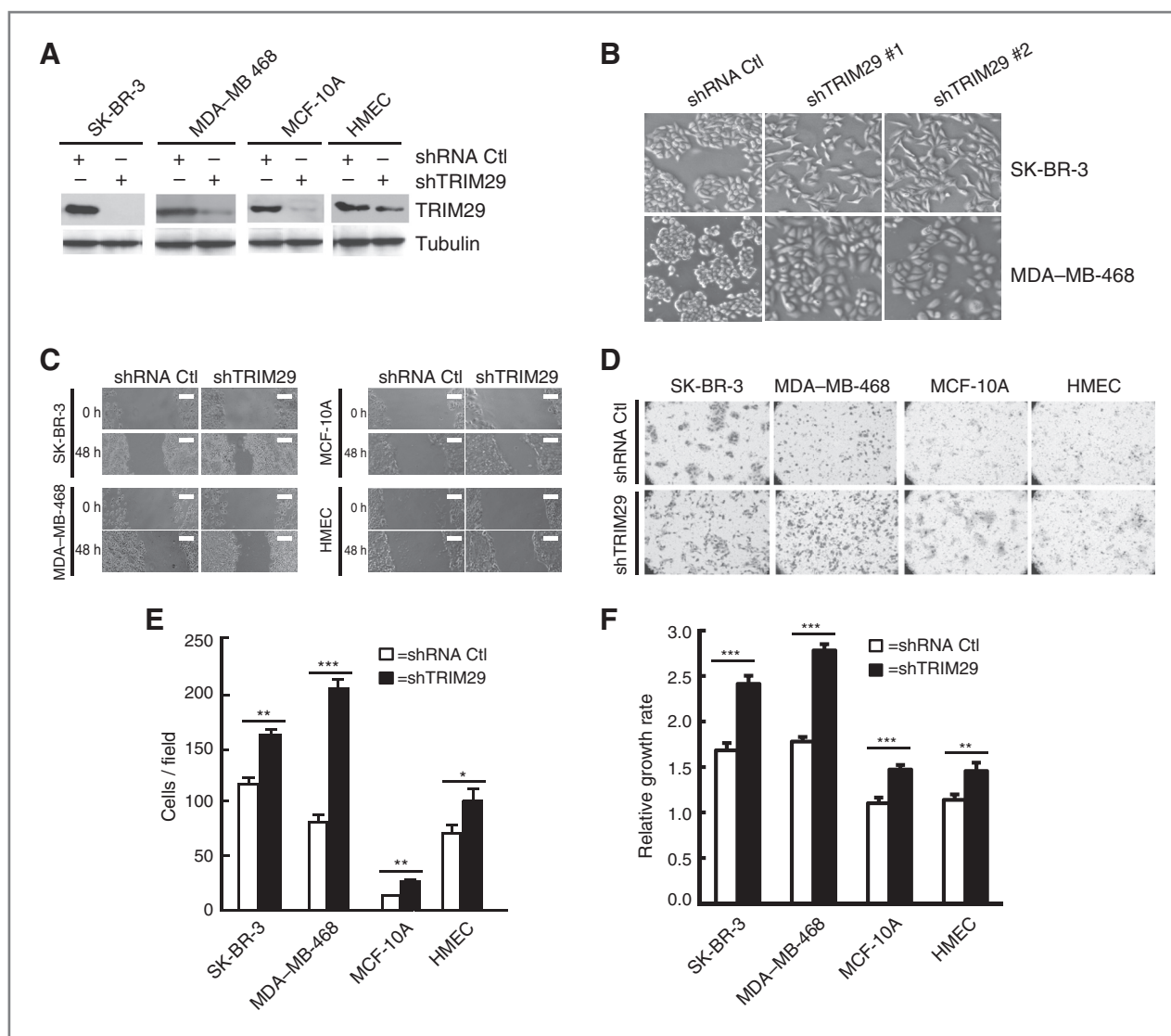


Figure 3. TRIM29 knockdown in breast tumor and control lines increases cell motility, invasiveness, and growth. **A**, SK-BR-3, MDA-MB-468, MCF-10A, and HMEC cells were transduced with lentivirus prepared from empty pLKO.1 plasmid (shRNA Ctl) or plasmid encoding a TRIM29-specific shRNA sequence (shTRIM29) and following selection were immunoblotted with anti-TRIM29 or tubulin. **B**, representative phase-contrast images of SK-BR-3 and MDA-MB-468 cells transduced with shRNA Ctl or two independent shTRIM29 vectors (#1 and #2). Note that these two different breast cancer cell lines show similar cell morphology changes (a mesenchymal-like phenotype) when TRIM29 is knocked down with two independent shRNAs. **C**, cultures were wounded with a pipette tip and photographed directly (0 hours) and 48 hours after wounding; scale bar, 350 μ m. **D**, representative micrographs of control and TRIM29 knockdown cells that have invaded through a Matrigel membrane. **E**, invaded cells were counted in control (open bars) and TRIM29 knockdown (filled bars) lines in 10 randomly chosen fields, the average of cells per field is graphed. **F**, relative growth rates of control (open bars) and TRIM29 knockdown (filled bars) lines were determined using CellTiter-Blue Reagent; error bars, 1.0 SE; *, $P < 0.05$; **, $P < 0.01$, ***, $P < 0.001$, Student t test.

in TRIM29 protein (Fig. 5D). Similarly, we measured a dose-dependent increase in TRIM29 transcript in SK-BR-3 and MDA-MB-468 cells after TWIST1 knockdown with siRNA (Fig. 5E and F, respectively). Because N-cadherin is a direct transcriptional target of TWIST1 (30), we also analyzed SK-BR-3 cells for expression of this gene following TWIST1 knockdown. The results indicate TWIST1 knockdown resulted in a significant dose-dependent decrease in N-cadherin mRNA abundance in SK-BR-3 (Fig. 5E). Similar results were obtained when control and TRIM29 shRNA knockdown SK-BR-3 cells were transfected with TWIST1 siRNA (Supplementary Fig. S4),

supporting the conclusion that TWIST1 is driving N-cadherin expression following TRIM29 knockdown.

We obtained a luciferase reporter plasmid (pGL3-Twist-Luc) containing a segment of the human *TWIST1* promoter (31). We observed when cotransfected with recombinant TRIM29 into HEK-293T cells that luciferase activity was decreased compared with cells cotransfected with reporter and control (pcDNA3.1) vector (Fig. 5G), suggesting that TRIM29 antagonizes transcription of the *TWIST1* gene. TWIST1 reporter assays conducted in SK-BR-3 and MDA-MB-468 cells indicated a significant increase in reporter

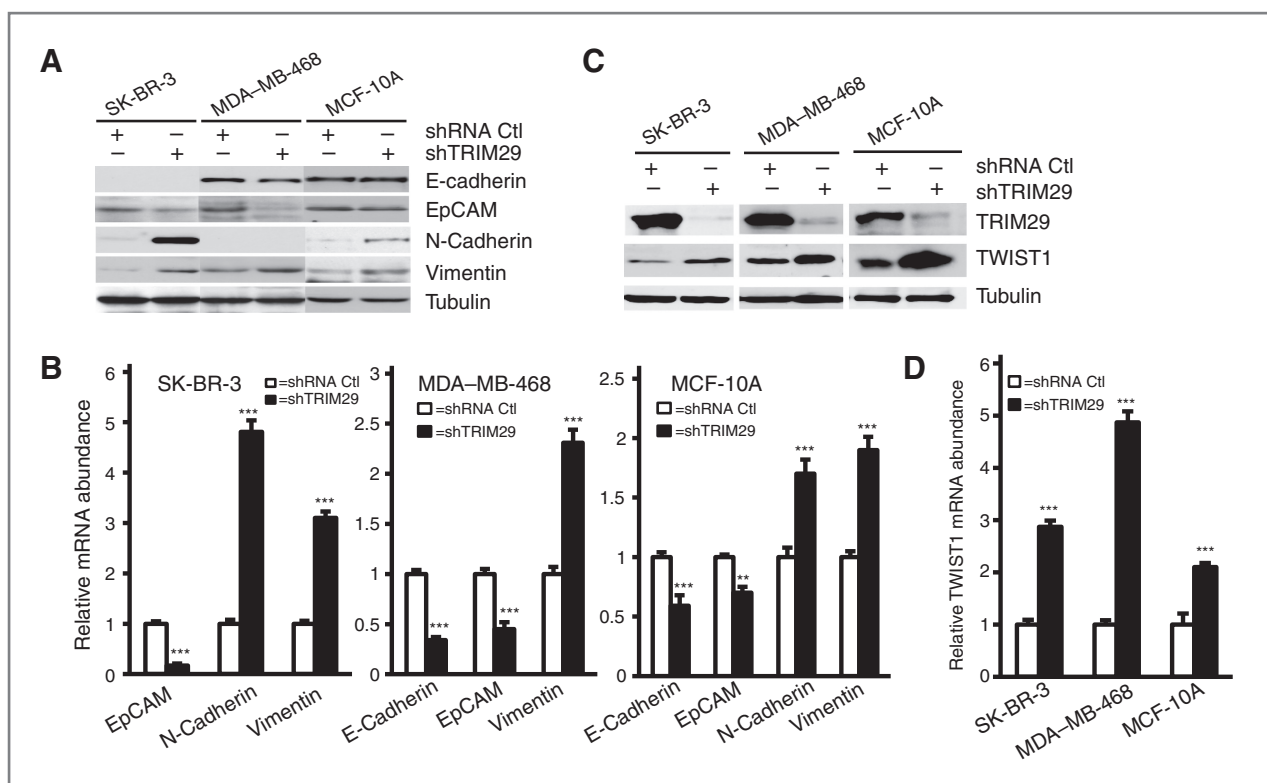


Figure 4. TRIM29 knockdown alters gene-expression patterns and increased expression of TWIST1. A, indicated control and TRIM29 knockdown lines were immunoblotted for E-cadherin, EpCAM, N-cadherin, vimentin, and tubulin. B, qRT-PCR analysis of relative mRNA abundance of indicated marker genes in control (open bars) and TRIM29 knockdown (filled bars) lines. C, immunoblot analysis of TWIST1, TRIM29, and tubulin in indicated control and TRIM29 knockdown cell lines. D, relative TWIST1 transcript abundance was measured in indicated control (open bars) and TRIM29 knockdown (filled bars) cell lines; error bars, 1.0 SE; **, $P < 0.01$; ***, $P < 0.001$, Student t test.

activity following TRIM29 knockdown (Fig. 5H). We conclude that TRIM29 and TWIST1 antagonize the activity and/or expression of each other, implying the presence of a novel negative feedback loop.

TWIST1 inhibits TRIM29 promoter activity

Inspection of the 5' flank of the human *TRIM29* gene revealed the presence of 10 canonical E-box sequences (5'-CANNTG-3') within a cluster upstream of the transcriptional start site (TSS) of the *TRIM29* gene (nt# -349 to -747; Fig. 6A). We amplified a 1,100-bp fragment of the *TRIM29* proximal promoter and cloned it into a luciferase-linked reporter plasmid (pGL3-Basic). When this construct (pTRIM29-Luc) was transfected into HEK-293T cells, we measured a multifold increase in luciferase activity compared with controls (Fig. 6B), indicating that this segment possesses promoter activity. When pTRIM29-Luc reporter was cotransfected into HEK-293T along with recombinant TWIST1, we observed repressed luciferase activity (Fig. 6B). We also measured decreased *TRIM29* reporter activity in both SK-BR-3 and MDA-MB-468 TRIM29 knockdown lines cells compared with controls (Fig. 6C), indicating that reduced TRIM29 protein levels decrease transcriptional activity of the *TRIM29* gene. Taken together, these results imply that TWIST1 represses *TRIM29* promoter activity.

We next used ChIP to analyze the association of recombinant TWIST1 with a segment of the *TRIM29* promoter containing multiple E-boxes (see Fig. 6A). To conduct these experiments, we transiently expressed HA-tagged human TWIST1 in SK-BR-3 and MDA-MB-468 cells with and without TRIM29 knockdown (Fig. 6D). qPCR measured significantly increased relative enrichment of the targeted locus in chromatin precipitated using anti-HA compared with chromatin precipitated with nonspecific mouse IgG (Fig. 6E), indicating interaction of recombinant TWIST1 with the targeted region of the *TRIM29* gene. Furthermore, increases in relative enrichment of HA-TWIST1 interaction with *TRIM29* were measured in chromatin harvested from TRIM29 knockdown SK-BR-3 and MDA-MB-468 cells (Fig. 6E), suggesting that reduced TRIM29 protein was allowing increased association of TWIST1 with the *TRIM29* gene.

We also stably expressed recombinant FLAG-tagged human TRIM29 in two breast tumor lines (BT-549 and MDA-MB-231) that have silenced endogenous TRIM29 expression, and HA-TWIST1 was expressed for the purpose of conducting ChIP (Fig. 6D). ChIP assays indicated that expression of recombinant TRIM29 protein resulted in a significant reduction in relative enrichment of the *TRIM29* promoter segment compared with cells not expressing recombinant TRIM29 (Fig. 6F), indicating reduced TWIST1 association with the *TRIM29* gene in the

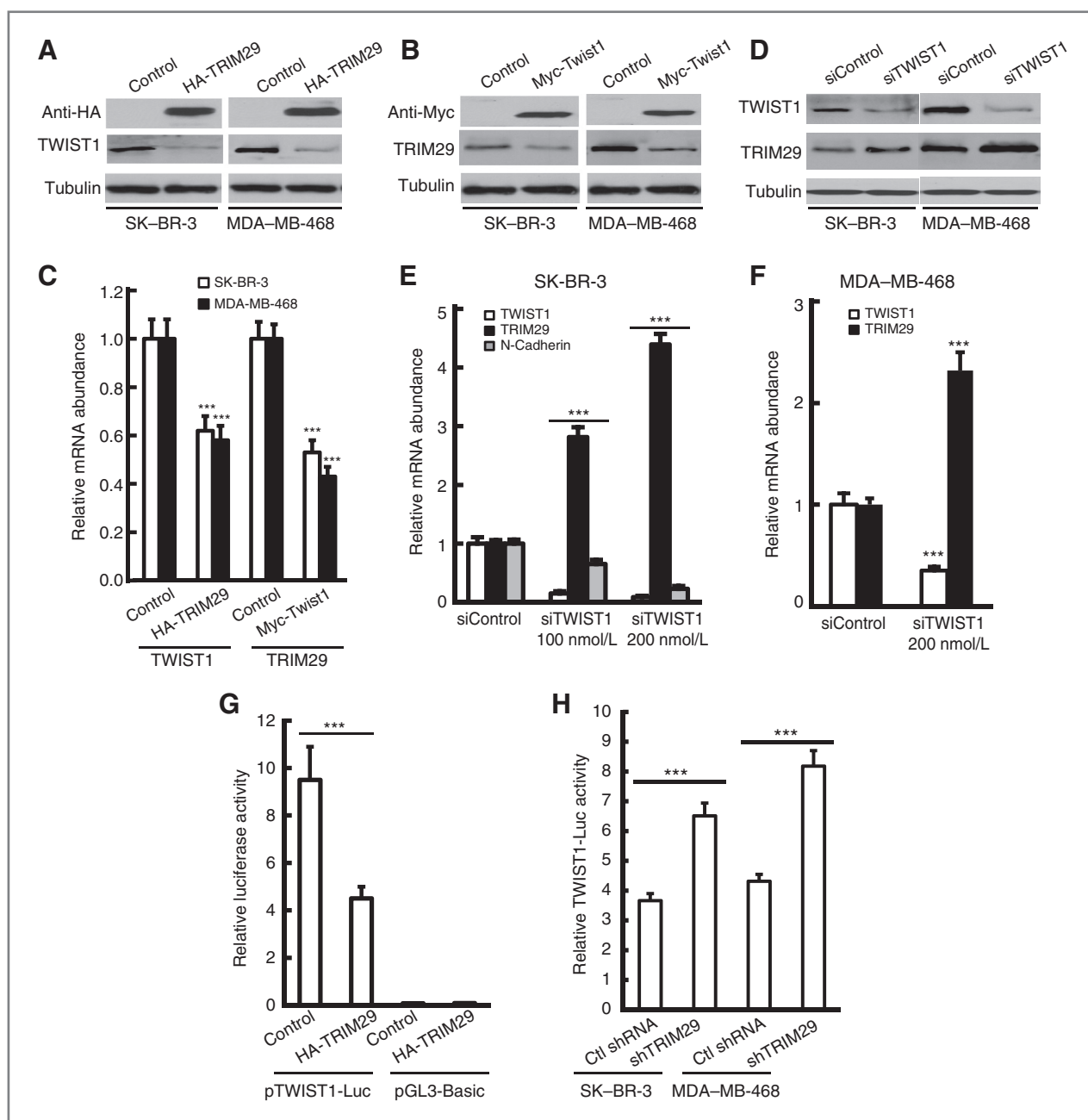


Figure 5. TWIST1 and TRIM29 exhibit a reciprocal relationship. A, SK-BR-3 or MDA-MB-468 cells were transiently transfected with empty pcDNA 3.1 (control) or plasmid encoding HA-tagged TRIM29 and immunoblotted with anti-HA, TWIST1, or tubulin. B, SK-BR-3 or MDA-MB-468 cells were transiently transfected with Myc-GFP-pCS3 (control) or plasmid encoding Myc-tagged Twist1. Lysates were immunoblotted with anti-Myc, TRIM29, or tubulin. C, SK-BR-3 (open bars) and MDA-MB-468 (filled bars) cells were transfected with respective control plasmid, plasmid encoding HA-tagged TRIM29 or Myc-tagged Twist1. Forty-eight hours posttransfection cells were harvested, RNA isolated, and analyzed by qRT-PCR for TWIST1 or TRIM29 mRNA abundance. D, SK-BR-3 or MDA-MB-468 cells were transfected with 200 nmol/L control (siControl) or TWIST1-specific siRNA (siTWIST1) and 48 hours posttransfection cells were harvested, lysed, and immunoblotted for TWIST1, TRIM29, or tubulin. E, SK-BR-3 cells were transfected with control, 100 nmol/L, or 200 nmol/L TWIST1-specific siRNA, and 48 hours posttransfection cells harvested, total RNA isolated, and qRT-PCR conducted to analyze TWIST1 (open bars), TRIM29 (filled bars), or N-cadherin (shaded bars) mRNA abundance. F, MDA-MB-468 cells were transfected with control or TWIST1-specific siRNA and qRT-PCR conducted to analyze TWIST1 (open bars) or TRIM29 (filled bars) mRNA abundance. G, HEK-293T cells were transfected with either pGL3-TWIST1-Luc or empty pGL3-Basic, and cotransfected with either pcDNA 3.1 (control) or plasmid encoding HA-tagged TRIM29. Lysates were measured for both firefly and *Renilla* luciferase and relative firefly luciferase signal calculated. H, control and TRIM29 knockdown SK-BR-3 and MDA-MB-468 cells were transfected with pGL3-TWIST1-Luc and 24 hours posttransfection the relative luciferase signal was measured; error bars, 1.0 SE; ***, $P < 0.001$, Student t test).

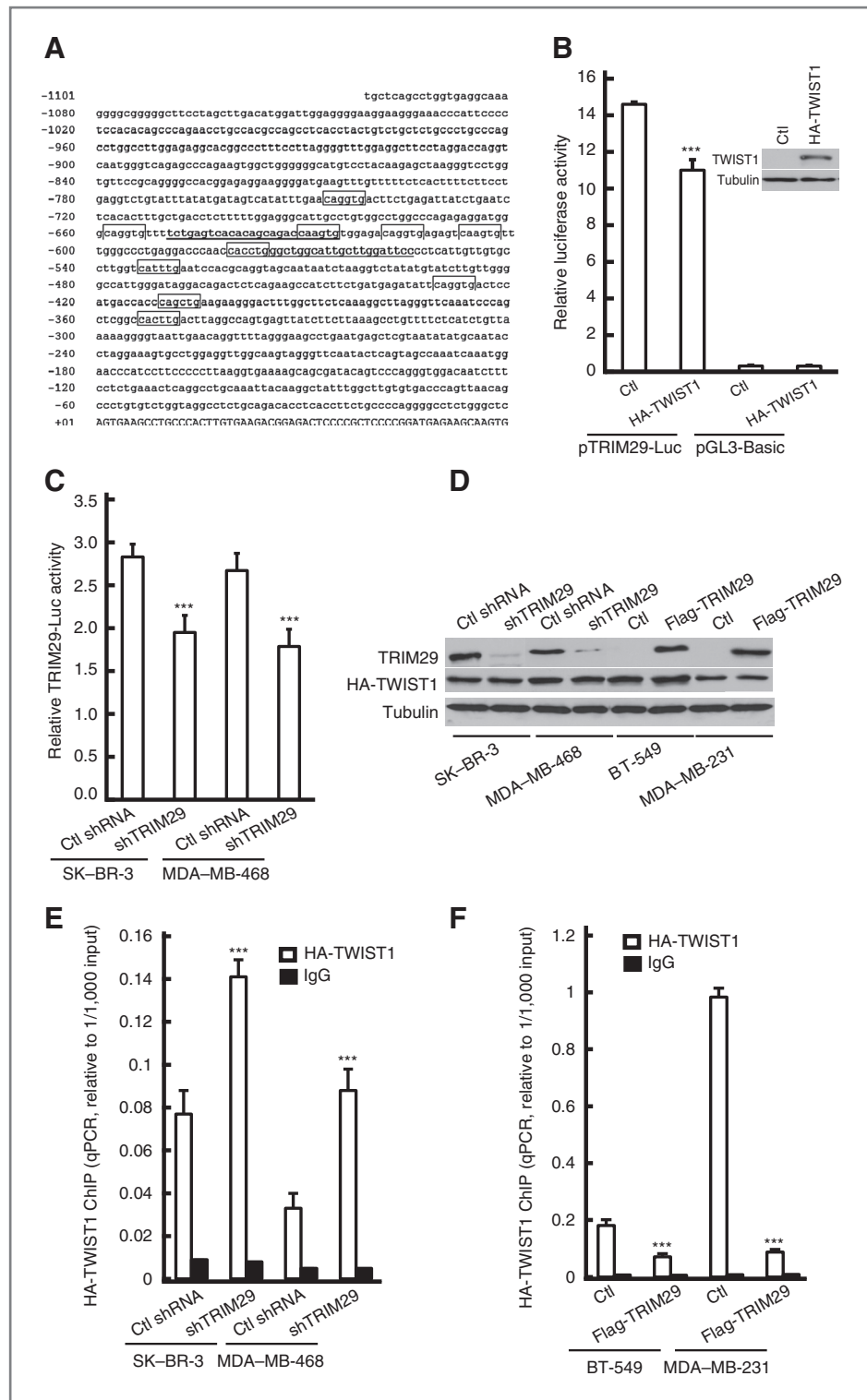


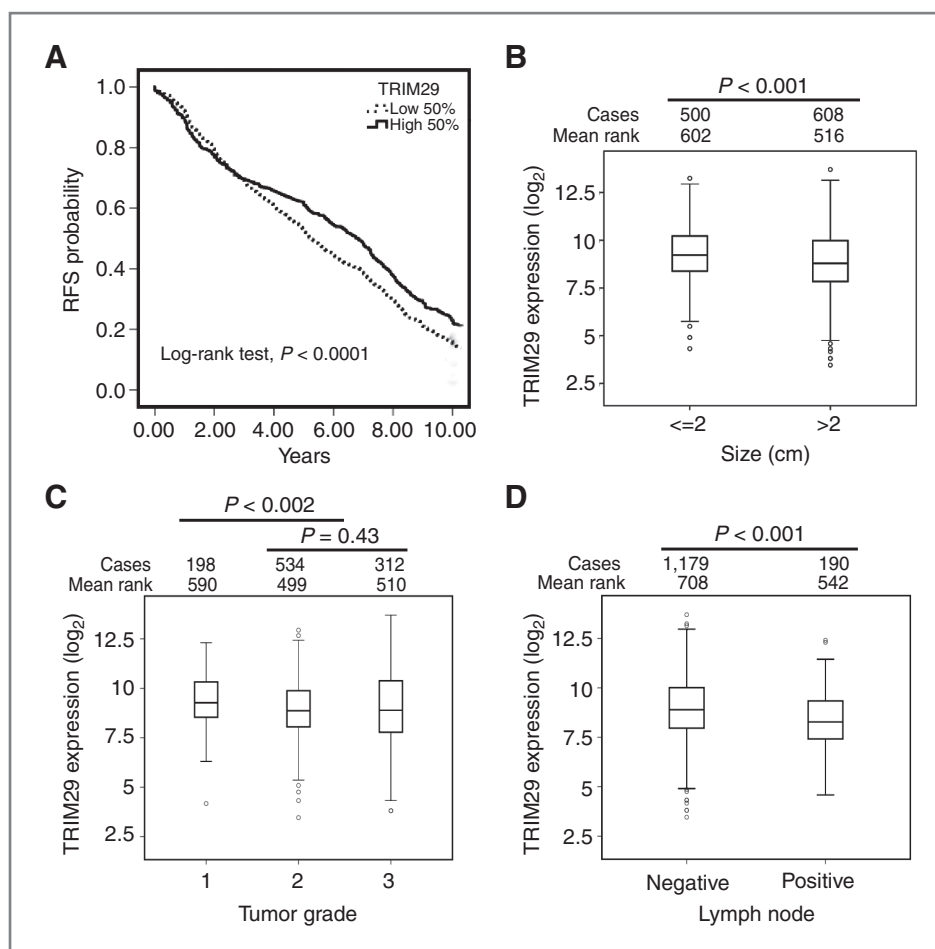
Figure 6. TWIST1 associates with the TRIM29 promoter and represses its activity. **A**, sequence of the 5' flank of the human *TRIM29* gene. Illustrated is the TSS (nt # +01); canonical E-box elements are boxed; location of primers used in ChIP are underlined. **B**, pTRIM29-Luc or pGL3-Basic was cotransfected into HEK-293T along with plasmid encoding recombinant HA-TWIST1 or empty pDNA 3.1 (Ctl). Inset, immunoblot showing transient TWIST1 expression in cells transfected with indicated plasmid. **C**, SK-BR-3 and MDA-MB-468 cells with and without TRIM29 knockdown were transfected with pTRIM29-Luc and relative luciferase activity measured 24 hours posttransfection. **D**, SK-BR-3 and MDA-MB-468 cells with and without TRIM29 knockdown, or BT-549 and MDA-MB-231 control cells or those stably expressing Flag-tagged TRIM29 were transiently transfected with a plasmid encoding HA-tagged TWIST1. Cell extracts were assayed by immunoblotting with anti-TRIM29, anti-HA, and anti-tubulin. **E**, chromatin was harvested from HA-TWIST1-expressing SK-BR-3 and MDA-MB-468 cells with and without TRIM29 knockdown and ChIP was conducted with anti-HA (open bars) or nonspecific mouse IgG (filled bars) and qPCR performed. **F**, chromatin was harvested from HA-TWIST1-expressing BT-549 and MDA-MB-231 control and Flag-tagged TRIM29-expressing cells. Chromatin was immunoprecipitated with anti-HA (open bars) or nonspecific mouse IgG (filled bars) and qPCR conducted; error bars, 1.0 SE; ***, $P < 0.001$, Student *t* test).

presence of TRIM29 protein. In sum, these findings indicate that TWIST1 associates (either directly or indirectly) with the *TRIM29* gene, this interaction is associated with transcriptional repression of the *TRIM29* gene, and that TRIM29 blocks the interaction of TWIST1 with the *TRIM29* gene.

Low TRIM29 expression is associated with reduced breast cancer patient survival and markers of aggressive breast cancer behavior

We used breast cancer data within the KM-Plotter database (32) to investigate the association of TRIM29 expression with

Figure 7. Reduced TRIM29 expression is associated with poorer survival and more aggressive breast cancer behavior. A, a public breast cancer database was queried to examine the association between patient with breast cancer RFS and *TRIM29* gene expression. Indicated is a log-rank *P* value, $n = 1,809$. TRIM29 expression (\log_2 values) was compared in breast tumors grouped by indicated size (B), tumor grade (C), and lymph node metastasis (D). The number of cases in each group is given as well as the calculated mean rank and *P* value (Mann-Whitney test).



breast cancer survival. This analysis indicated that low TRIM29 expression was significantly ($P < 0.0001$) associated with reduced relapse-free survival (RFS) compared with patients with higher TRIM29 expression (Fig. 7A). Of note, we found no significant association between TRIM29 expression and overall survival in this set of patients with breast cancer.

Comparison of breast tumors ≤ 2 cm with tumors > 2 cm indicated that the TRIM29 expression is significantly lower in the larger tumors (Fig. 7B). We also observed that higher-grade (Grades 2 and 3) tumors displayed significantly lower TRIM29 expression compared with grade 1 tumors (Fig. 7C). Of note, we found no significant difference when TRIM29 expression was compared between grade 2 and grade 3 tumors ($P = 0.43$, Mann-Whitney test). Lower TRIM29 expression was also associated with tumors positive for lymph node spread compared with node-negative tumors (Fig. 7D). Independent of either patient age at diagnosis, lymph node status, tumor size or grade, or estrogen receptor (ER) expression, low TRIM29 expression was found to be a significant predictive factor for reduced RFS in patients with breast cancer when multivariate survival analysis using a Cox model was applied to this dataset (Supplementary Fig. S5A–S5E and Supplementary Table S2). In sum, low TRIM29 expression is associated with reduced RFS, more aggressive

tumor characteristics (increased tumor size and grade), and metastatic breast cancer behavior.

Discussion

Iacobuzio-Donahue and colleagues observed that TRIM29 expression was approximately 5-fold elevated in primary pancreatic tumors and cell lines compared with normal pancreas or duodenal mucosa (11). Later, it was determined that when included in a six-gene panel, elevated TRIM29 expression could distinguish pancreatic ductal adenocarcinoma from chronic pancreatitis (33). Recent reports indicate that TRIM29 overexpression is commonly observed in squamous cell carcinoma and non-small cell lung cancers (9, 10) and in 69% (86/124) of gastric cancer cases as judged by qRT-PCR (8). Of note, these investigators also documented that elevated TRIM29 expression is associated with aggressive gastric tumor characteristics and reduced patient survival.

In contrast, Nacht and colleagues (34) observed that TRIM29 was underexpressed by at least 10-fold in approximately 50% of primary breast tumors compared normal mammary tissue. We have documented, in both cultured cells and primary breast tumors, that the *TRIM29* gene is a novel target for epigenetic silencing. Thus, it is likely that the reduced TRIM29 expression

measured in this earlier study was attributable, at least in part, to aberrant DNA hypermethylation within the *TRIM29* gene.

The notion that TRIM29 could function in a potentially tumor-suppressive role in breast cancer was first suggested when Hosoi and colleagues (23) documented that expression of recombinant TRIM29 in BT-549 cells suppressed both colony-forming ability and proliferation. Expression of recombinant TRIM29 in MCF7 cells also slowed growth rates and reduced anchorage-independent growth (14), and we have observed similar effects in BT-549 and MDA-MB-231 cells (data not shown). Conversely, knockdown of TRIM29 in MCF-10A cells promoted anchorage-independent growth, increased cell motility and invasiveness, and disrupted 3D acinar formation *in vitro* (14). We have confirmed these findings using a broader panel of breast tumor and mammary epithelium-derived cell lines, and extended these studies by determining that knockdown of TRIM29 in breast cancer cells altered gene-expression patterns in a manner consistent with increased cell motility and invasiveness. In sum, available evidence firmly supports the conclusion that TRIM29 functions in a growth/invasion-suppressive capacity in mammary epithelial cells.

We observed that patients with breast cancer with tumors exhibiting reduced TRIM29 expression have reduced RFS. Furthermore, low TRIM29 expression is associated with more aggressive tumor features. Liu and colleagues (14) observed reduced survival in young women with ER⁺ tumors, but reported no difference in older women with ER⁺ breast cancer. Analysis of the database used in our study revealed that low TRIM29 expression was significantly associated with poorer RFS regardless of patient age at diagnosis (Supplementary Fig. S5A). Although clearly in need of further analysis and data refinement, these facts suggest that TRIM29 expression may be useful as a prognostic breast cancer biomarker.

Our study of breast cancer cells with TRIM29 knockdown indicated that concomitant with reduced TRIM29 expression was a coordinate increase in TWIST1, a bHLH transcription factor that, like other bHLH proteins (i.e., SNAIL, SLUG, ZEB1, and ZEB2), functions in an oncogenic role in breast cancer (35). Specifically, transcription factors of this subgroup promote the epithelial-to-mesenchymal transition (EMT) during cancer progression. EMT is an embryonic program that governs cell motility and, accordingly, TWIST1 is critical for closure of the neural tube during embryogenesis (36). In the context of cancer, activation of EMT promotes otherwise nonmotile and polarized epithelial cells to lose polarity and cell-cell contact, and invade adjacent stroma (29). For this reason, increased TWIST1 activity is associated with metastatic activity (35). As our study demonstrates that TRIM29 suppresses TWIST1 expression and activity, we conclude that this activity is at least one mechanism by which TRIM29 functions to suppress breast cancer development.

We observed that TRIM29 knockdown results in upregulation of TWIST1 and, conversely, that expression of TRIM29 drives down TWIST1 levels in cultured breast cancer cells. These findings suggest that TRIM29 has an inhibitory role on the transcription of the TWIST1 gene. Furthermore, expression of recombinant TRIM29 resulted in reduced association of TWIST1 with the *TRIM29* gene as judged by ChIP. These findings imply that TRIM29 interferes with the function of the TWIST1

protein. At present, we are unsure of the mechanism(s) that underlie these observations. As TRIM29 antagonizes p53 function by sequestering this transcription factor in the cytoplasm (13), it is tempting to speculate that TRIM29 could be functioning in a parallel role to sequester factor(s) that promote TWIST1 transcription. Alternatively, although TRIM29 has been characterized as a cytoplasmic protein (3) and has not been reported to interact with chromatin, it contains two B-box Zn-finger motifs and other B-box proteins are transcriptional modulators, generally as components of protein complexes (37).

Knockdown of TWIST1 resulted in increased TRIM29 mRNA and protein levels and expression of recombinant TWIST1 had the opposite effect. Inspection of genomic sequence revealed a cluster of 10 canonical E-box elements upstream of the TRIM29 TSS and expression of recombinant TWIST1 resulted in measurable suppression of transcription of a reporter driven by a portion of the TRIM29 proximal promoter containing this E-box cluster. ChIP analysis confirmed that TWIST1 associates with a segment of the TRIM29 promoter containing several of these E-box elements. Others have recently reported that TWIST1 binds to E-boxes within the *ESR1* (ER α) gene, leading to the transcriptional repression of ER α (38), and our work supports the conclusion that TWIST1 similarly functions to suppress expression of the *TRIM29* gene in breast cancer cells.

In summary, we document that the *TRIM29* gene is a novel target for epigenetic silencing in breast cancer and that knockdown of the TRIM29 protein results in alterations in gene-expression patterns that drive increased cell growth, motility, and invasiveness. We also document that TRIM29 suppresses the activity of the oncogenic transcription factor TWIST1, providing a molecular basis for the emerging view that TRIM29 is a potential tumor suppressor in breast cancer.

Disclosure of Potential Conflicts of Interest

No potential conflicts of interest were disclosed.

Authors' Contributions

Conception and design: L. Ai, K.D. Brown

Development of methodology: L. Ai, W.-J. Kim, K.D. Brown

Acquisition of data (provided animals, acquired and managed patients, provided facilities, etc.): W.-J. Kim, M. Alpay, M. Tang, C.E. Pardo, C.D. Heldermon, E.M. Siegel

Analysis and interpretation of data (e.g., statistical analysis, biostatistics, computational analysis): L. Ai, M. Alpay, M. Tang, E.M. Siegel, K.D. Brown

Writing, review, and/or revision of the manuscript: C.D. Heldermon, E.M. Siegel, K.D. Brown

Administrative, technical, or material support (i.e., reporting or organizing data, constructing databases): L. Ai, S. Hatakeyama, W.S. May, M.P. Kladd

Study supervision: K.D. Brown

Acknowledgments

The authors thank Drs. Seto, Maestro, and Wang for their generous gifts of plasmid constructs used in this study.

Grant Support

This work was supported by funding from the Florida Department of Health and NIH (1R03CA143980; E.M. Siegel and K.D. Brown). M. Alpay was supported by funding from the Turkish Government.

The costs of publication of this article were defrayed in part by the payment of page charges. This article must therefore be hereby marked *advertisement* in accordance with 18 U.S.C. Section 1734 solely to indicate this fact.

Received December 12, 2013; revised June 11, 2014; accepted June 11, 2014; published OnlineFirst June 20, 2014.

References

- Short KM, Cox TC. Subclassification of the RBCC/TRIM superfamily reveals a novel motif necessary for microtubule binding. *J Biol Chem* 2006;281:8970–80.
- Hatakeyama S. TRIM proteins and cancer. *Nat Rev Cancer* 2011;11:792–804.
- Reymond A, Meroni G, Fantozzi A, Merla G, Cairo S, Luzi L, et al. The tripartite motif family identifies cell compartments. *EMBO J* 2001;20:2140–51.
- Napolitano LM, Meroni G. TRIM family: pleiotropy and diversification through homomultimer and heteromultimer formation. *IUBMB Life* 2012;64:64–71.
- Ozato K, Shin DM, Chang TH, Morse HC III. TRIM family proteins and their emerging roles in innate immunity. *Nat Rev Immunol* 2008;8:849–60.
- Fristrup N, Birkenkamp-Demtroder K, Reinert T, Sanchez-Carbayo M, Segersten U, Malmstrom PU, et al. Multicenter validation of cyclin D1, MCM7, TRIM29, and UBE2C as prognostic protein markers in non-muscle-invasive bladder cancer. *Am J Pathol* 2013;182:339–49.
- Glebov OK, Rodriguez LM, Soballe P, DeNobile J, Cliatt J, Nakahara K, et al. Gene expression patterns distinguish colonoscopically isolated human aberrant crypt foci from normal colonic mucosa. *Cancer Epidemiol Biomarkers Prev* 2006;15:2253–62.
- Kosaka Y, Inoue H, Ohmachi T, Yokoe T, Matsumoto T, Mimori K, et al. Tripartite motif-containing 29 (TRIM29) is a novel marker for lymph node metastasis in gastric cancer. *Ann Surg Oncol* 2007;14:2543–9.
- Tang ZP, Dong QZ, Cui QZ, Papavassiliou P, Wang ED, Wang EH. Ataxia-telangiectasia group D complementing gene (ATDC) promotes lung cancer cell proliferation by activating NF-kappaB pathway. *PLoS ONE* 2013;8:e63676.
- Xiao Z, Jiang Q, Willette-Brown J, Xi S, Zhu F, Burkett S, et al. The pivotal role of IKKalpha in the development of spontaneous lung squamous cell carcinomas. *Cancer Cell* 2013;23:527–40.
- Iacobuzio-Donahue CA, Ashfaq R, Maitra A, Adsay NV, Shen-Ong GL, Berg K, et al. Highly expressed genes in pancreatic ductal adenocarcinomas: a comprehensive characterization and comparison of the transcription profiles obtained from three major technologies. *Cancer Res* 2003;63:8614–22.
- Wang L, Heidt DG, Lee CJ, Yang H, Logsdon CD, Zhang L, et al. Oncogenic function of ATDC in pancreatic cancer through Wnt pathway activation and beta-catenin stabilization. *Cancer Cell* 2009;15:207–19.
- Yuan Z, Villagra A, Peng L, Coppola D, Glozak M, Sotomayor EM, et al. The ATDC (TRIM29) protein binds p53 and antagonizes p53-mediated functions. *Mol Cell Biol* 2010;30:3004–15.
- Liu J, Welm B, Boucher KM, Ebbert MT, Bernard PS. TRIM29 functions as a tumor suppressor in nontumorigenic breast cells and invasive ER⁺ breast cancer. *Am J Pathol* 2012;180:839–47.
- Ai L, Kim WJ, Demircan B, Dyer LM, Bray KJ, Skehan RR, et al. The transglutaminase 2 gene (TGM2), a potential molecular marker for chemotherapeutic drug sensitivity, is epigenetically silenced in breast cancer. *Carcinogenesis* 2008;29:510–8.
- Livak KJ, Schmittgen TD. Analysis of relative gene expression data using real-time quantitative PCR and the 2(-Delta Delta C(T)) Method. *Methods* 2001;25:402–8.
- Ai L, Kim WJ, Kim TY, Fields CR, Massoll NA, Robertson KD, et al. Epigenetic silencing of the tumor suppressor cystatin M occurs during breast cancer progression. *Cancer Res* 2006;66:7899–909.
- Demircan B, Dyer LM, Gerace M, Lobenhofer EK, Robertson KD, Brown KD. Comparative epigenomics of human and mouse mammary tumors. *Genes Chromosomes Cancer* 2009;48:83–97.
- Darst RP, Pardo CE, Ai L, Brown KD, Klade MP. Bisulfite sequencing of DNA. *Curr Protoc Mol Biol* 2010;9:1–17.
- Sho T, Tsukiyama T, Sato T, Kondo T, Cheng J, Saku T, et al. TRIM29 negatively regulates p53 via inhibition of Tip60. *Biochim Biophys Acta* 2011;1813:1245–53.
- Kim WJ, Gersey Z, Daaka Y. Rap1GAP regulates renal cell carcinoma invasion. *Cancer Lett* 2012;320:65–71.
- Ai L, Skehan RR, Saydi J, Lin T, Brown KD. Ataxia-telangiectasia, mutated (ATM)/nuclear factor kappa light chain enhancer of activated B cells (NFkappaB) signaling controls basal and DNA damage-induced transglutaminase 2 expression. *J Biol Chem* 2012;287:18330–41.
- Hosoi Y, Kapp LN, Murnane JP, Matsumoto Y, Enomoto A, Ono T, et al. Suppression of anchorage-independent growth by expression of the ataxia-telangiectasia group D complementing gene, ATDC. *Biochem Biophys Res Commun* 2006;348:728–34.
- Gardiner-Garden M, Frommer M. CpG islands in vertebrate genomes. *J Mol Biol* 1987;196:261–82.
- Robertson KD. DNA methylation and human disease. *Nat Rev Genet* 2005;6:597–610.
- Hampton GM, Mannermaa A, Winqvist R, Alavaikko M, Blanco G, Taskinen PJ, et al. Loss of heterozygosity in sporadic human breast carcinoma: a common region between 11q22 and 11q23.3. *Cancer Res* 1994;54:4586–9.
- Thiery JP. Epithelial-mesenchymal transitions in tumour progression. *Nat Rev Cancer* 2002;2:442–54.
- Hiraguri S, Godfrey T, Nakamura H, Graff J, Collins C, Shayesteh L, et al. Mechanisms of inactivation of E-cadherin in breast cancer cell lines. *Cancer Res* 1998;58:1972–7.
- De Craene B, Berx G. Regulatory networks defining EMT during cancer initiation and progression. *Nat Rev Cancer* 2013;13:97–110.
- Alexander NR, Tran NL, Rekapally H, Summers CE, Glackin C, Heimark RL. N-cadherin gene expression in prostate carcinoma is modulated by integrin-dependent nuclear translocation of Twist1. *Cancer Res* 2006;66:3365–9.
- Cheng GZ, Zhang WZ, Sun M, Wang Q, Coppola D, Mansour M, et al. Twist is transcriptionally induced by activation of STAT3 and mediates STAT3 oncogenic function. *J Biol Chem* 2008;283:14665–73.
- Gyorffy B, Lanczky A, Eklund AC, Denkert C, Budczies J, Li Q, et al. An online survival analysis tool to rapidly assess the effect of 22,277 genes on breast cancer prognosis using microarray data of 1,809 patients. *Breast Cancer Res Treat* 2010;123:725–31.
- Chen Y, Zheng B, Robbins DH, Lewin DN, Mikhitarian K, Graham A, et al. Accurate discrimination of pancreatic ductal adenocarcinoma and chronic pancreatitis using multimarker expression data and samples obtained by minimally invasive fine needle aspiration. *Int J Cancer* 2007;120:1511–7.
- Nacht M, Ferguson AT, Zhang W, Petroziello JM, Cook BP, Gao YH, et al. Combining serial analysis of gene expression and array technologies to identify genes differentially expressed in breast cancer. *Cancer Res* 1999;59:5464–70.
- Yang J, Mani SA, Donaher JL, Ramaswamy S, Itzykson RA, Come C, et al. Twist, a master regulator of morphogenesis, plays an essential role in tumor metastasis. *Cell* 2004;117:927–39.
- Chen ZF, Behringer RR. twist is required in head mesenchyme for cranial neural tube morphogenesis. *Genes Dev* 1995;9:686–99.
- Torok M, Etkin LD. Two B or not two B? Overview of the rapidly expanding B-box family of proteins. *Differentiation* 2001;67:63–71.
- Vesuna F, Lisok A, Kimble B, Domek J, Kato Y, van der Groep P, et al. Twist contributes to hormone resistance in breast cancer by down-regulating estrogen receptor-alpha. *Oncogene* 2012;31:3223–34.

Cancer Research

The Journal of Cancer Research (1916–1930) | The American Journal of Cancer (1931–1940)

TRIM29 Suppresses TWIST1 and Invasive Breast Cancer Behavior

Lingbao Ai, Wan-Ju Kim, Merve Alpay, et al.

Cancer Res 2014;74:4875-4887. Published OnlineFirst June 20, 2014.

Updated version Access the most recent version of this article at:
doi:[10.1158/0008-5472.CAN-13-3579](https://doi.org/10.1158/0008-5472.CAN-13-3579)

Supplementary Material Access the most recent supplemental material at:
<http://cancerres.aacrjournals.org/content/suppl/2014/06/24/0008-5472.CAN-13-3579.DC1>

Cited articles This article cites 38 articles, 14 of which you can access for free at:
<http://cancerres.aacrjournals.org/content/74/17/4875.full.html#ref-list-1>

Citing articles This article has been cited by 3 HighWire-hosted articles. Access the articles at:
[/content/74/17/4875.full.html#related-urls](http://cancerres.aacrjournals.org/content/74/17/4875.full.html#related-urls)

E-mail alerts [Sign up to receive free email-alerts](#) related to this article or journal.

Reprints and Subscriptions To order reprints of this article or to subscribe to the journal, contact the AACR Publications Department at pubs@aacr.org.

Permissions To request permission to re-use all or part of this article, contact the AACR Publications Department at permissions@aacr.org.